AIAA AVIATION Forum
5-9 June 2017, Denver, Colorado
18th AIAA/ISSMO Multidisciplinary Analysis and Optimization Conference

AIAA 2017-4148

Design of an Unmanned Aerial Vehicle for Long-Endurance Communication Support

Berk Ozturk*, Michael Burton*, Ostin Zarse†,
Warren Hoburg‡, Mark Drela§, John Hansman§

A long-endurance, medium-altitude unmanned aerial vehicle (UAV) was designed to provide communication support to areas lacking communication infrastructure. Current solutions involve larger, more costly aircraft that carry heavier payloads and have maximum flight durations of less than 36 hours. The presented design would enable a 5.6 day mission with a 10 lb, 100 W communications payload, providing coverage over an area 100 km in diameter. A geometric program was used to size the aircraft, which is a piston-engine unmanned aircraft with a 24 ft wingspan, and a takeoff weight of 147 lbs. The airframe is designed to be modular, which allows for fast and easy transportation and assembly for an operating crew of four to six. The aircraft can station-keep in 90% of global wind conditions at an altitude of 15,000 ft.

Nomenclature

ADS-B	Automatic Dependent Surveillance-Broadcast
BLOS	beyond line-of-slight
BSFC	brake specific fuel consumption
CG	center of gravity
GP	geometric program
ECU	engine control unit
FAA	Federal Aviation Administration
FAR	Federal Aviation Regulations
GPS	Global Positioning System
IC	internal combustion
LOS	line-of-sight
MSL	mean sea level
MTOW	maximum takeoff weight
PMU	power management unit
RC	remote control
RPM	revolutions per minute
STP	standard temperature and pressure
UAV	unmanned aerial vehicle
UHF	ultra-high frequency

I. Introduction

UAVs are regularly deployed with communications payloads to provide support to ground operations. One example is in disaster relief zones where the existing communication system has been disabled. The Air Force currently uses UAVs such as the RQ-4 Global Hawk to loiter over communication support zones to enable long-distance communications between ground units. These aircraft have high initial costs, high operating costs ($18,900/hour[1]), and endurance capabilities of less than 36 hours.

Developments in small and light communications payloads create an opportunity to redesign the aircraft that deliver them. We propose a design for a gas-powered, 24 ft wingspan, medium-altitude UAV better suited to these new payloads, shown in Figure 1. The aircraft has a takeoff weight of 147 pounds, a fuel fraction of 59%, and is capable of loitering at up to 15,000ft over the communication support zone for up to 5.6 days while carrying a 10 pound, 100 W communications payload. This paper discusses the concept of operations for the aircraft, the driving requirements of the design, the optimization procedure, and the performance of the aircraft in different operational scenarios.

*Graduate Student, MIT, Department of Aeronautics and Astronautics.
†Undergraduate Student, MIT, Department of Aeronautics and Astronautics.
‡Assistant Professor, MIT, Department of Aeronautics and Astronautics. AIAA Member.
§Professor, MIT, Department of Aeronautics and Astronautics. AIAA Member.

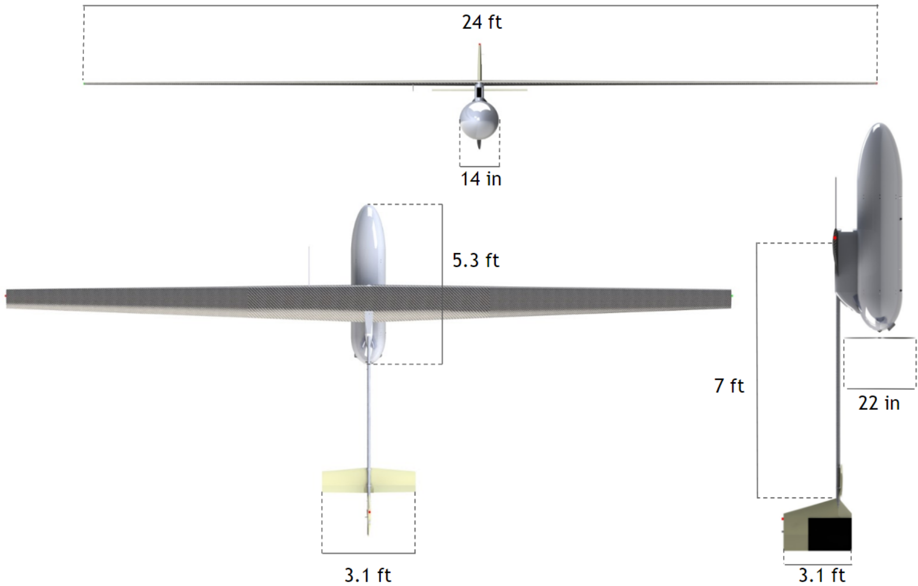

Figure 1: Dimensional overview of the aircraft

II. Concept of Operations

The concept of operations detailed in this section informs the mission requirements for the aircraft. The operational strategy of the aircraft was conceived by considering the important features of an aircraft deployed for disaster relief. Many of the procedures within the concept of operations have been adapted from common UAV control procedures.

Before deployment for communication support, the disassembled aircraft is stored in a 108"x24"x22" container and ready for shipment. Two smaller containers hold the ground station equipment and the required launch mechanism. In the case of a natural disaster, the three containers are sent to a launch location within 200 nmi of the communication support zone.

When the three containers arrive at the launch location, a small ground crew of four to six assemble the aircraft, the ground station, and the launch mechanism in parallel. The launch mechanism shown in Figure 2 is a metal frame used to support the UAV on the roof of a launch vehicle, such as a car or pick-up truck, to allow for a vehicle-assisted launch. The ground team secures the launch mechanism to the launch vehicle and then loads the dry aircraft onto the launch mechanism. The ground team then performs avionics and systems checks and fills the fuel tanks.

Figure 2: The aircraft is mounted on the back of a launch vehicle, which brings the aircraft to rotation speed.

Takeoff is performed within visual range of a ground-based pilot who has direct control of the aircraft through a UHF controller included with the ground station. The launch vehicle, driven by an operator, accelerates to the aircraft's rotation speed. When rotation speed is reached, the pilot performs a pull-up

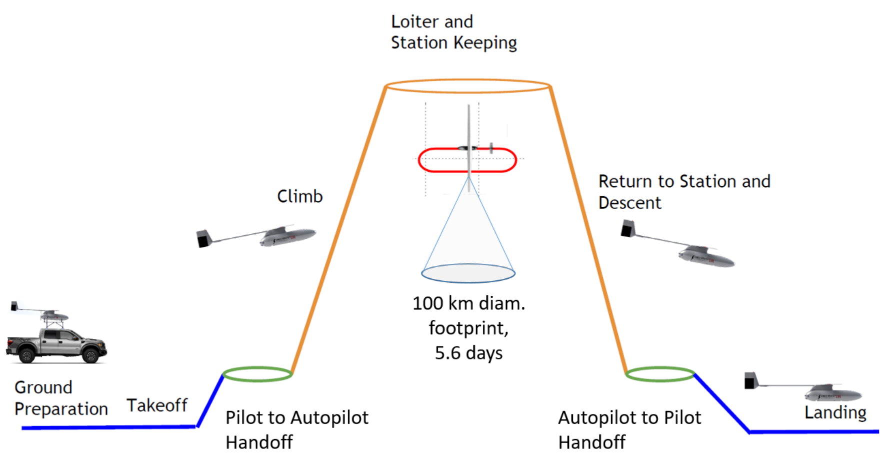

Figure 3: Concept mission profile

maneuver to allow the aircraft to separate from the vehicle. The aircraft launch requires less than 1050 ft of straight road (paved or unpaved) for takeoff, considering the acceleration and braking distance of typical vehicles.

After takeoff, the ground-based pilot transfers control authority of the aircraft to the autopilot system. The aircraft autonomously climbs to the loiter altitude of 15,000 ft. The aircraft then cruises to the communication support zone. Upon arrival, the aircraft follows a waypoint system to autonomously loiter for a minimum of 5 days.

The aircraft's payload provides a communication link between ground units that are beyond line-of-sight (BLOS) from each other. Communication between the aircraft and its operators is maintained through a satellite-based Internet system, which allows operators to receive telemetry data regarding the aircraft's systems.

In the last stage of its mission, the aircraft autonomously cruises back to its landing location, and the ground-based pilot visually lands the aircraft using the UHF radio.

After landing, the ground team performs the necessary maintenance. The aircraft is able to launch within 6 hours if more communication coverage is required. Multiple aircraft can be coordinated to provide more persistent coverage or cover adjacent sectors. If the aircraft's mission has concluded, all of the components of the aircraft system are packed and shipped back to its storage location to await its next mission.

III. Requirements

Table 1 lists the requirements of the aircraft that fulfill the concept of operations described in Section II.

Table 1: The set of requirements for the proposed long-endurance communication support aircraft.

Requirement	Specification
Endurance	> 5 days
Communications coverage area	100 km diameter with a minimum ground elevation angle of 5°
Station-keeping	Maintain coverage in $> 90\%$ of wind conditions globally
Range to/from station	200 nmi
Payload	10lb weight, 100W electrical power draw, 1ft^3 volume

IV. Requirements Analysis

This section explains how each requirement directly influences the aircraft design.

A. Endurance

The design of the aircraft is primarily driven by the endurance requirement. The endurance requirement is 5 days (120 hours). The current endurance record for a gas-powered UAV belongs to the Aurora Orion, which flew for 80 hours in 2014.[2] As such, the proposed aircraft will be operating at the upper limits of current gas-piston aircraft technology.

An analysis on the feasibility of solar powered aircraft to satisfy the requirements was conducted in the early stages of this aircraft's development. With the worst-case operational scenario being high-wind conditions in the winter solstice, it was concluded that a solar aircraft cannot achieve the requirement for station-keeping with current technology. In contrast, a gas-powered aircraft is not subject to time of year and latitude operational restrictions. Thus, the proposed aircraft design is powered by a piston engine.

For loitering aircraft, endurance is maximized by minimizing power consumption, which requires flying at low airspeeds. However, the aircraft has to fly faster than the windspeed at a given altitude to station-keep. This means that the loiter speed of the aircraft does not necessarily correspond to its maximum endurance speed, as would be expected from a conventional maximum endurance aircraft design.

B. Communications Coverage and Station-Keeping

The communication coverage area requirement determines the aircraft's minimum loitering altitude because the payload uses LOS communication. Taking into account the curvature of Earth, maintaining a minimum 100 km footprint with a minimum ground elevation angle of 5° requires flight at 4.6 km (15,000 ft) above ground level.

Different altitudes require different propulsive capabilities because of changes in air density and mean wind speeds. As shown in Figure 4, the 90th percentile wind at 4.6km (shown by the bounding line h_{min}) is 25 m/s. It is estimated that normally-aspirated, piston-engine aircraft can operate at altitudes up to 7 km. Theoretically, high endurance aircraft could also operate at higher altitudes (>20,000 m), where there exists a local minimum in wind speeds. However, higher altitude operations require a turbocharger or supercharger, which add cost, weight, and risk to the aircraft design.

In the altitude range between 4.6 km and 7 km, wind speed increases linearly. Since lower wind speeds are beneficial for higher endurance, an operating altitude of 4.6km (15,000 ft) was selected to satisfy the requirements while minimizing takeoff weight. At this operating altitude, the aircraft will have to operate at a minimum loiter speed of 25 m/s to satisfy the station-keeping requirement.

C. Implicit Requirements

Aircraft modularity is implicitly required in order to allow for easy shipping of the aircraft to its launch location. And while aircraft cost is not a specified requirement, the aircraft must be cost effective. Studies have shown that aircraft cost is proportional to aircraft weight.[3] For this aircraft, minimizing maximum takeoff weight (MTOW) as an objective will result in lower operational and unit costs. With alternative missions in mind, the ability to accommodate various payload sizes, power loads, and weights are all beneficial as well.

V. Vehicle Sizing and Optimization

There were important multidisciplinary trade-offs that needed to be understood in order to correctly size the proposed aircraft. To explore these trade-offs, an optimization tool called GPkit was used. GPkit is a convex optimization framework that leverages Geometric Programming (GP).[4]

A. Geometric Programming Overview

GP is a special form of optimization in which the constraints of the aircraft system are expressed in monomial and posynomial forms.[5] The general form of a GP problem is shown in Equation 1,

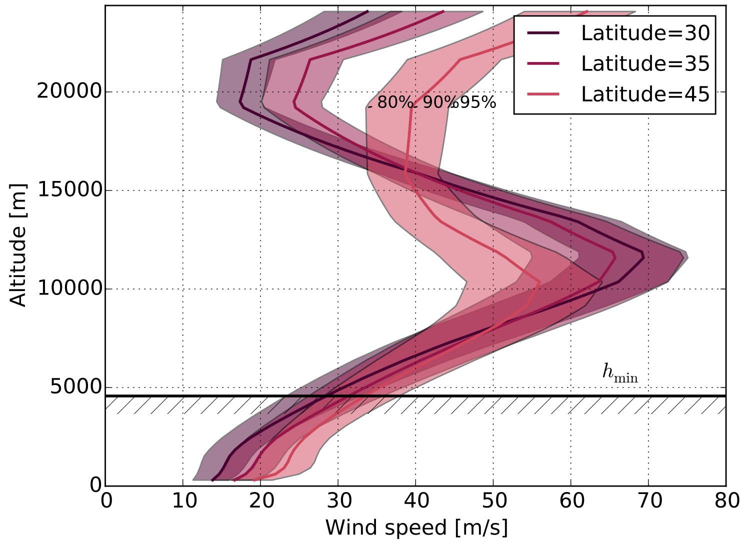

Figure 4: The global 80th, 90th and 95th percentile winds as functions of altitude. The lower-bounding line shows the minimum loiter altitude of 4.6km (15,000 ft.)

$$
\begin{aligned}
\text{minimize } & f_0(\mathbf{x}) \\
\text{subject to } & f_i(\mathbf{x}) \leq 1, i = 1, ..., m \\
& g_i(\mathbf{x}) = 1, i = 1, ..., p
\end{aligned}
\tag{1}
$$

where the functions f_i must be *posynomial* functions and the functions g_i must be *monomial* functions. *Posynomials* and *monomials* have the forms

$$
f(\mathbf{x}) = \sum_{k=1}^{K} c_k x_1^{a_{1_k}} x_2^{a_{2_k}} \cdots x_n^{a_{n_k}}, \tag{2}
$$

$$
g(\mathbf{x}) = c x_1^{a_1} x_2^{a_2} \cdots x_n^{a_n}. \tag{3}
$$

GPs present significant advantages in solution reliability, speed, and modularity of constraints and objectives compared to other optimization formulations. GPs require no initial guesses or parameter tuning to obtain globally optimal solutions given a set of GP constraints. Sparse GPs with thousands of variables and constraints can be solved in fractions of a second. The set of constraints, models and objective functions are easy to modify within GPkit, and can provide insight about the Pareto frontier of the trade space. The dual solution of a GP, which is an output of solving the GP, provides gradient information in the form of sensitivities to different design parameters to help engineers understand the impact of assumptions and constraints on the performance of a design.

This optimization framework allows for the coupled design of all subsystems of the aircraft. In the design of the UAV, each subsystem (aerodynamics, structures, propulsion, avionics, operations) contributed different models and governing equations specific to their discipline. These models were converted into the GP-compatible forms aforementioned, and were integrated systematically into the optimization model.

B. Configuration Overview

The assumed configuration for the GP models is a fixed-wing aircraft with a conventional tail. The aircraft structure consists primarily of composites. A single-cylinder internal combustion engine drives the propeller and the alternator, generating thrust and electrical power for the avionics and payload. The vehicle has a pylon-mounted wing, with an integrated engine intake for both aspiration and cooling. The vehicle can be remotely piloted, or operated autonomously via autopilot. Figure 5 overviews the notable design features of the aircraft.

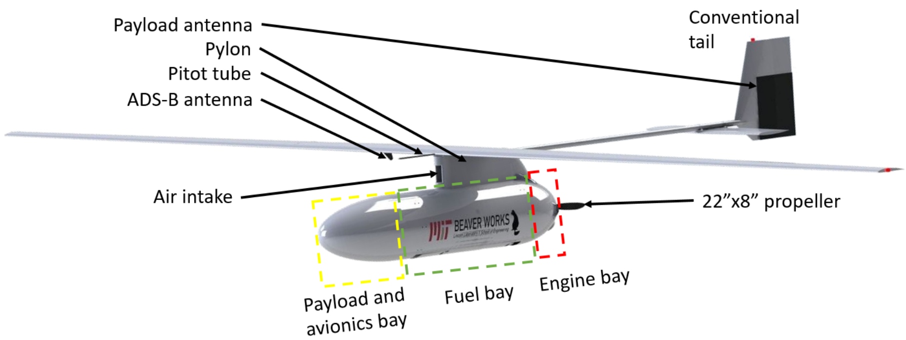

Figure 5: Notable design features of the aircraft

A pusher configuration was selected to eliminate the effects of scrubbing drag, and to allow for unobstructed payload and sensor mounting in the nose of the aircraft, which has a volume of 1.43 cubic-feet. Traditional landing gear configurations were foregone for a shock-absorbing rear landing wheel and a forward landing skid because analysis showed that the weight and drag added by a tricycle landing gear would have increased the fuel required to achieve the 6 day mission endurance by up to 17%. This decision required the design of a non-traditional, effective landing and takeoff system.

The aircraft uses a vehicle-assisted takeoff procedure, described in Section II. For landing, the front landing skid and the rear wheel dissipate the vertical kinetic energy of the impact by compressing shock-absorbing rubber stoppers through a stroke distance. The wing tips of the aircraft are reinforced to be able to withstand a wingtip strike.

There are implicit requirements for the aircraft from an operations perspective. The potential for the vehicle to be deployed around the world necessitates modularity and ease of transport. Analysis on the modularity of the design was done post-optimization, and is presented in Figure 21 in Section XI. This allows the packaged aircraft, its ground station and launch systems to be transported around the world within 24 hours, ready to be deployed in a moment's notice.

C. Modeling Assumptions

The following are the assumptions used in the design optimization of the proposed aircraft, along with a brief justification.

1. Mission Profile:

The mission profile (also outlined in Section II) starts with a climb to 15,000ft. Throughout the climb phase, the aircraft climbs at a rate of at least 100 ft/min. The aircraft then cruises 200 nmi to the communication support zone. While loitering, the aircraft provides a communication coverage footprint of 100 km for a minimum of 5 days. Then it cruises back to its point of takeoff. The plane was modeled to be in steady flight during all phases of the mission.

2. Engine Weight, Power, and Propeller Efficiency:

The engine size and available engine power were based off a power-law regression fit[6] to a dataset of two and four stroke, gas piston engines. Figure 6 shows the weight and power distribution of the data used in the regression.

Furthermore we assumed that the engine BSFC performance at different throttle levels could be approximated by the curve shown in Figure 7. Data provided by RCV Engines Ltd., a small reciprocating UAV engine company, was used to validate the model. The BSFC behavior with throttle level was especially important to model accurately. Since long endurance aircraft have high fuel mass fractions, they tend to

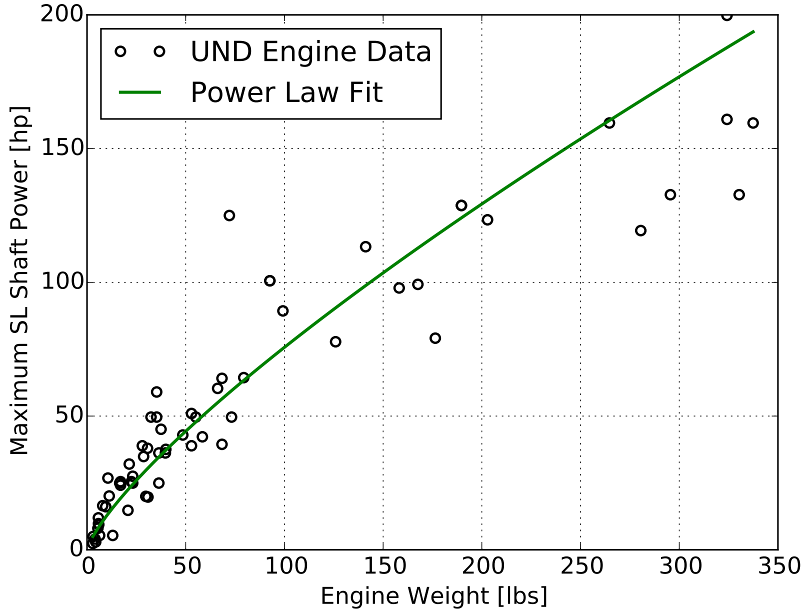

Figure 6: Weight versus power curve for small reciprocating engines.[7] The trendline is a monomial approximation of the available engine data.

throttle back towards the end of their missions as fuel is consumed. Throttling back has an associated BSFC penalty that is appropriately captured in the engine BSFC model shown in Figure 7.

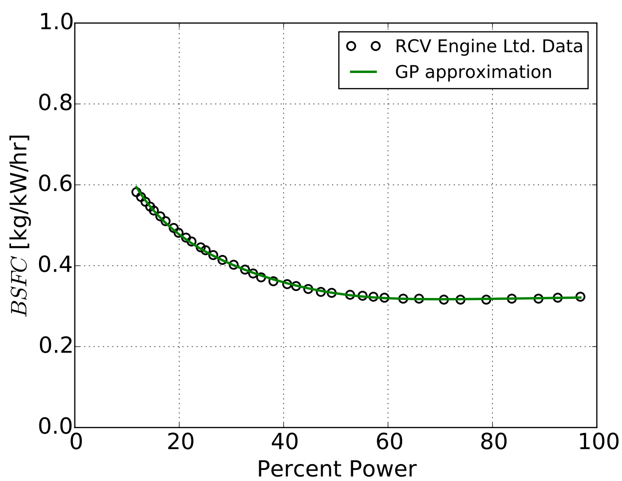

Figure 7: Comparison of GP approximation to DF70 power mapping.

The propeller efficiency was assumed to be constant during each phase of the mission, with a conservative average efficiency of 68% during loiter.

3. Aerodynamics

The wing is assumed to be manufactured out of three equal-span wing sections. It is a constant taper wing with a taper ratio of 0.5, which provides a compromise between structural weight and span efficiency. There is no dihedral built into the design. It is estimated that the tip deflection of the aircraft under loading, combined with its high-wing configuration, provide enough roll stability to make extra dihedral unnecessary.

The empennage of the aircraft has a conventional tail configuration. Configuration studies were conducted to see the relative performance of three different designs, namely an inverted-V tail, a pi tail, and dual dart tails. However, the potential interference of the payload patch antenna with the aircraft's carbon fiber structure and engine necessitated the placement of the antenna on the vertical tail, as shown in Figure 5. This placed constraints on the minimal dimensions of the vertical tail, which resulted in the conventional tail design outperforming the other concepts. The horizontal tail is sized for 100% CL margin for maximum forward CG of the aircraft (maximum payload of 25 lbs). The vertical tail is sized using a tail volume coefficient. The vertical tail has a small downward offset to reduce the interference of the antenna with the fuselage and to reduce the torsion loads on the tail boom, without causing potential tail-strikes during landing.

The set of control surfaces consists of an aileron on each side of the wing, two elevators on the horizontal tail, and a rudder on the vertical tail. The control surfaces are sized for sufficient control authority at V_{stall}, and the associated actuators are sized for maneuvers at the never-exceed speed of 40 m/s. The analysis for control surface loading was conducted using XFOIL.[8]

We assume that drag is a sum of the wing and tail profile drag, the induced drag, the fuselage drag, and the drag from the tail boom and the pylon, with added margins.

- **Wing and Tail Profile Drag:** The wing profile drag model was fitted[6] from drag polars of the JH01, JH02, and JH03 airfoils, created in XFOIL[8] (a two-dimensional computational fluid dynamics program), and is a function of the lift coefficient and Reynolds number. Figure 8 shows the airfoil drag polar used to calculate the wing profile drag. These airfoils are variants of the remote controlled (RC) glider airfoil SD7032 suitable for higher Reynolds number operation and a larger airfoil thickness ratio. The pressure distributions of the airfoils at maximum and minimum lift coefficients are shown in Figure 9. Similarly, the drag polar for the symmetric NACA0008 airfoil was used to calculate the profile drag of the tail surfaces.

- **Induced Drag:** The induced drag is calculated from the lift required by the aircraft, assuming a conservative span efficiency of 90%.

- **Fuselage Drag:** The fuselage was modeled in MTFLOW, an axisymmetric version of XFOIL, which gave a values for $C_{D_{fuselage}}$ of 0.0028 and 0.0032 for a laminar nose and a turbulent nose (tripped at the leading edge to ensure full turbulence) in the loiter condition, respectively. A Blasius turbulent flat plate model, with an associated form factor correction (fineness ratio of 6.5), is implemented in the GPkit model to extrapolate the drag coefficient to other flight conditions.

- **Other Sources of Drag:** The drag from the tail boom and the pylon have been modeled by a Blasius turbulent flat plate model, and are captured within C_{D_0}.

- **Drag Margin:** To account for other sources of drag (cooling drag, interference drag, manufacturing imperfections etc.) there is a 110% margin added to all non-wing sources of drag.

- **Total Vehicle Drag:** The total vehicle drag is the sum of the individual sources mentioned above:

$$C_D = C_{D_{\text{wing-profile}}} + \frac{C_L^2}{\pi e AR} + 2.1[C_{D_{\text{fuselage}}} + C_{D_{\text{tail}}} + C_{D_0}] \tag{4}$$

4. Avionics Weight and Volume:

We assume that the avionics weight is 8 lbs, occupies a volume of 0.125 cubic feet, and draws 65W of mean electrical power. We base the estimate on the avionics and batteries needed for actuators, ground communication, satellite communication, alternators, and flight control computers.

5. Structures

The structural design of this aircraft is driven by the need for a lightweight structure that is modular and allows for payload flexibility. The aircraft is designed with composite materials (Kevlar, carbon fiber, and fiberglass).

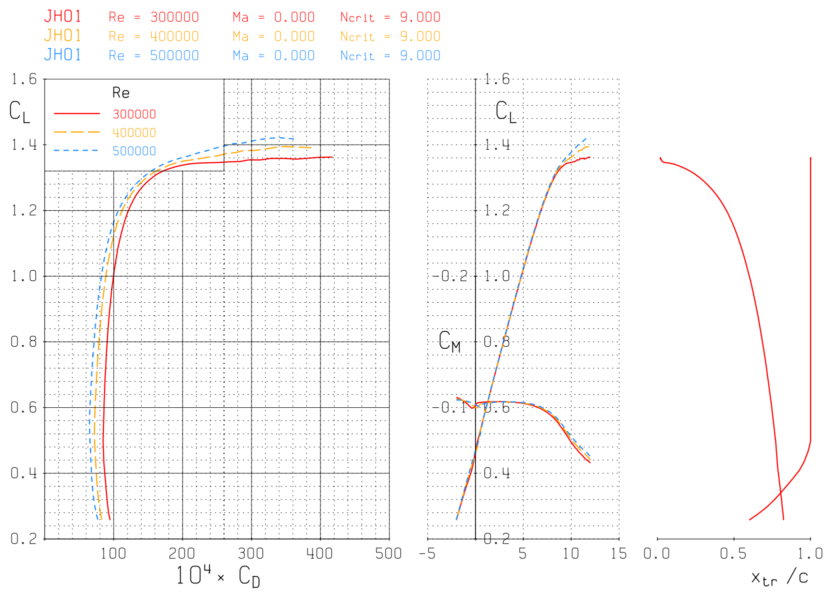

Figure 8: Drag polars for the JH01 airfoil at $Re = 3e5 - 5e5$

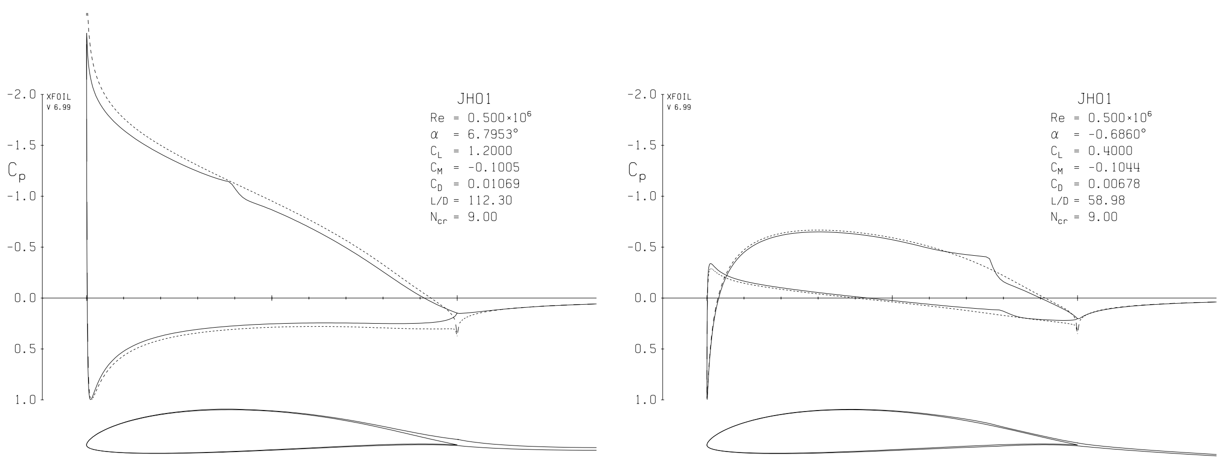

(a) Max Operating CL

(b) Min Operating CL

Figure 9: Pressure Distributions for the JH01 airfoil at maximum and minimum operating c_l

- **Wing:** The wing has a solid foam core construction, with carbon front and rear spars, and carbon skin. The spars are sized such that the front spar is capable of withstanding all the bending loads resulting from a 5 g pull-up maneuver with a maximum wing tip deflection that is less than 20% of the wingspan. The smaller rear spar is designed for in-plane bending loads. Since the main structural bending elements of the wing are the two carbon fiber spars, the aerodynamic skin is made with minimum gauge carbon.

- **Tail:** The tail is constructed from a solid foam core with a Kevlar skin, and a single spar for bending loads. The tail boom is sized by constraining the maximum deflection of the tip of the boom during maneuvers at the never-exceed speed of 40 m/s at MSL.

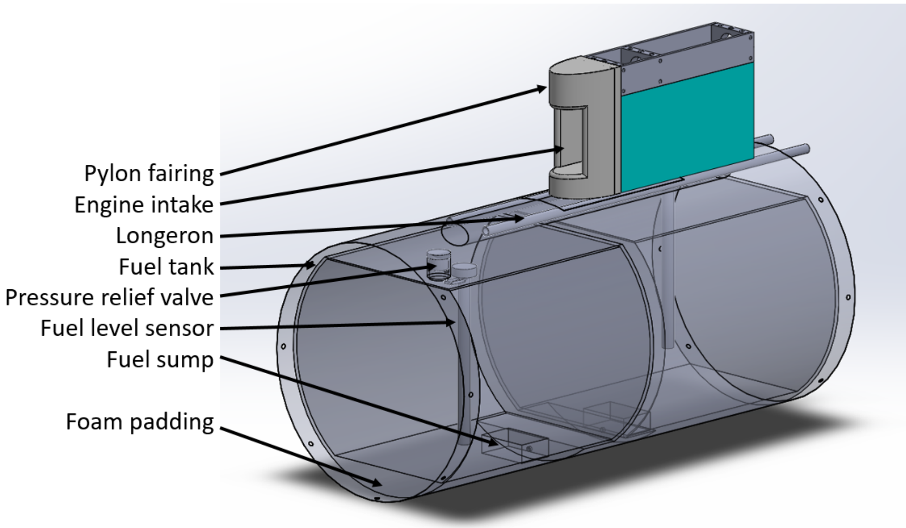

Figure 10: Fuselage layout. The carbon fiber skin has been made transparent to show internal structure.

- **Fuselage:** The fuselage is assumed to hold the payload, avionics, batteries, fuel tanks, and the propulsion system. The engineering drawing of the fuselage is shown in Figure 10. The important features of the fuselage are detailed below:
  - **Pylon:** The pylon contains the air intake and cooling duct, and transfers the aerodynamic loads from the wing and the tail into the fuselage. These loads are transferred into the structural shell of the fuselage through two longerons and a center bulkhead. A CAD of the proposed design is shown in Figure 11.

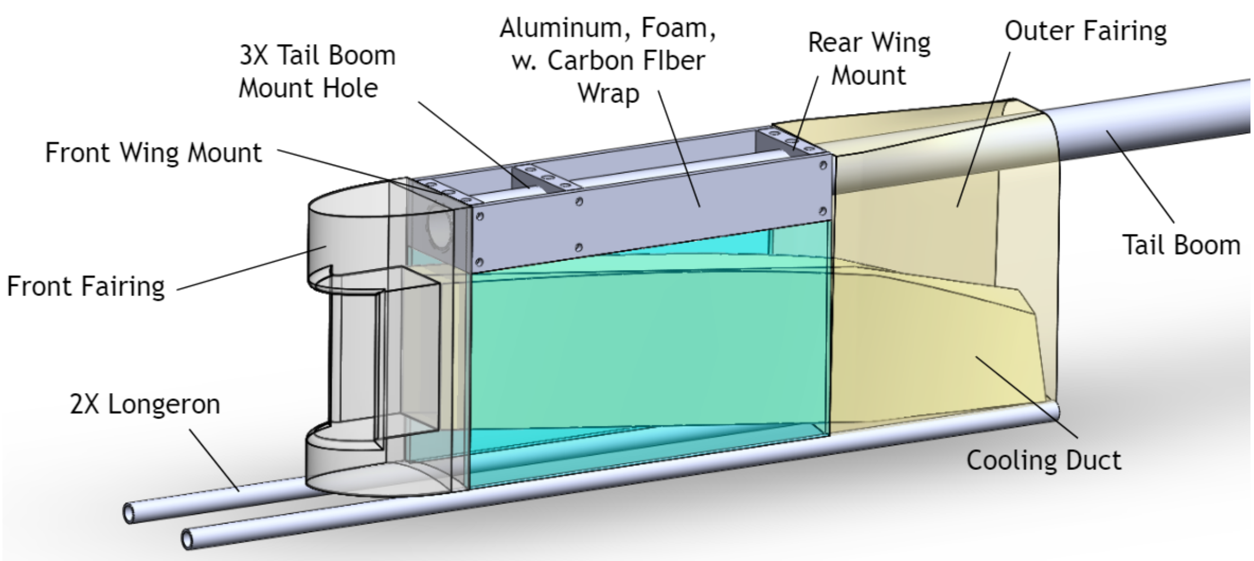

Figure 11: The pylon provides a structural connection between the wing, fuselage and tail, and houses the cooling duct.

  - **Fuel tanks:** The fuel tanks sit below the pylon, so that their CG is coincident to the aircraft's overall CG. The fuel volume has been separated into two bays to mitigate static stability issues that may result from fuel movement when the aircraft is pitched.

– **Rear landing wheel:** Underneath the rear bulkhead is a wheel which is the first point of contact of the aircraft upon landing, and is designed to absorb the loads experienced during a fully-fueled landing. The support structure is made of aluminum, and when it impacts the ground, compresses a rubber stopper that mitigates landing g-loads and dissipates the vertical kinetic energy of the aircraft. A diagram of the setup is shown in Figure 12.

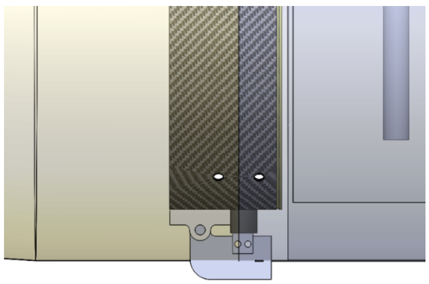

(a) Front landing gear is under the front bulkhead

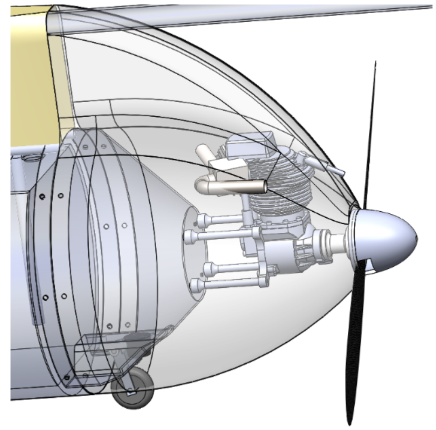

(b) Rear landing gear is nestled in the rear bulkhead and engine fairing

Figure 12: Landing gear and engine configuration of the aircraft. Rear fairing is transparent to show internals.

– **Front landing skid:** Underneath the front bulkhead is a blade which functions with the same principle as the rear wheel, absorbing the residual rotational kinetic energy of the aircraft post rear-wheel touchdown.

– **Engine bay:** The engine is mounted on the conical, carbon fiber rear bulkhead, as shown in Figure 12. The engine mount has been designed to mitigate engine vibrations, and also to accommodate the routing of the cooling duct into the engine.

– **Payload and avionics bay:** The front bulkhead functions as an avionics bay, and contains 0.125 cubic feet of electronics. The payload is mounted on the lid of the avionics bay.

– **Aerodynamic fairings:** The aerodynamic fairing around the payload is made of Kevlar, and the fairing around the engine is made with bidirectional carbon fiber. These components are made of minimum gauge material since they are not load-bearing. The components in the bays are mounted directly onto the bulkheads connecting to the structural fuselage shell.

VI. GPkit Optimization

From the above assumptions and margins, the sizing problem is defined by a set of constraints that govern the system. To be able to formulate the design as a geometric program, all of the constraints were expressed in monomial and posynomial forms. The objective function was set to maximize the time on station, with all design variables free, including the engine. Then, by varying MTOW it was observed how the time on station was affected by the size of the aircraft. Figure 13 shows the tradeoff of time on station versus MTOW.

While more time on station could be achieved with larger aircraft, there are various downsides to larger aircraft in manufacturability, modularity, complexity, risk and cost. The endurance requirement of 5 days falls on the Pareto Frontier shown in Figure 13.

The first-order aircraft size was determined through the trade study, but it was necessary to specify a commercially-available engine for a realistic aircraft sizing because of the limited number of options for compatible gas-piston engines with the appropriate power output. The TP70 engine, a 70 cc single-cylinder four-stroke engine, was selected. The TP70 has the necessary power for the operation of the aircraft during all segments of the flight (discussed further in Appendix B). Having chosen the engine, the aircraft was re-optimized for endurance with the engine parameters fixed.

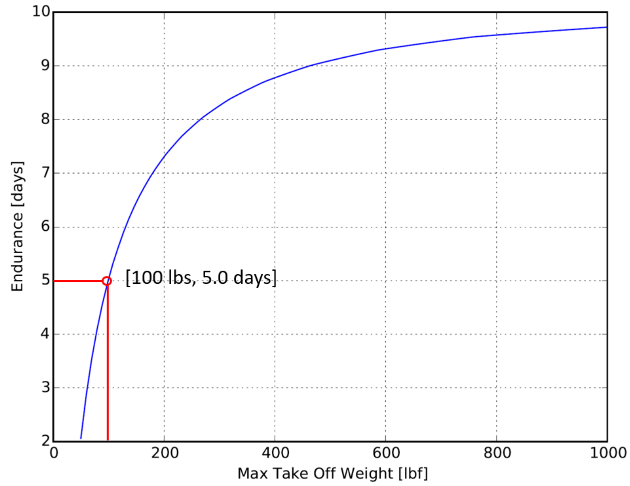

Figure 13: Trade-off between MTOW and the time on station. According to the models, an endurance of 5 days can be achieved by a 100 lb aircraft, assuming that all engine parameters are optimized.

VII. Aircraft Overview

The re-optimization discussed in Section VI results in the aircraft described in Figure 1. It is a 147 lb aircraft that is designed to fly for 5.6 days, and has a 59% fuel fraction. The weight breakdown of the components within the aircraft is outlined in Figure 14. Since the first version of the aircraft is being prototyped at MIT, both the budgeted and actual weights of each component are listed. The prototype aircraft is 2 lbs lighter than the budgeted total weight of 147 lbs.

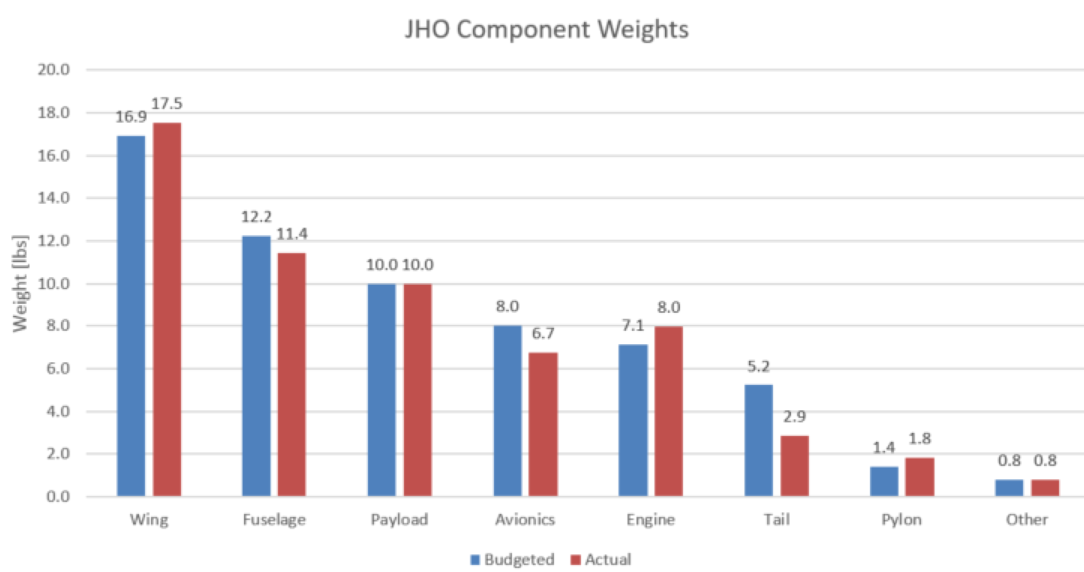

Figure 14: Budgeted and actual weights of subsystem components. Fuel has been omitted for graphical purposes, and weighs 86.3 lbs. The total weight of the components is 145 lbs, 2 lbs lighter than the 147 lbs projected by the GP models.

A. FAR107-Compliant Aircraft

In an effort to simplify flight testing, the MIT 16.82 Flight Vehicle Engineering Team has devised a version of the aircraft that has a total weight of less than 55lbs. Within Part 107 of the FAA Federal Aviation Regulations (FAR), this aircraft can be operated at altitudes less than 400 feet above ground level, within line-of-sight of an appropriately-trained, land-based pilot. There are further restrictions of the aircraft operations to daylight hours with more than 3 miles of visibility. The purpose of the FAR107-compliant aircraft will be to test flight-critical systems, including but not limited to controller tuning, autonomous operation, rate of fuel consumption, and engine and avionics cooling.

The aircraft weighs less than 55 lbs after the removal of the following components:

- Alternator: Since the prototype will be operating for short durations (<1 hr), the aircraft's electronics can be run on the on-board battery.
- Transponder and antenna: Satellite communications and the payload antenna are not required while in LOS flight.
- Communications payload: The payload is deemed unnecessary for preliminary flight system tests.
- Fuel tanks: The prototype will use a simple rigid fuel tank in the payload bay to save weight.

This configuration poses static margin challenges, since the removal of these components offsets the CG of the aircraft significantly aftward. To restore its longitudinal stability, the FAR107-compliant aircraft will have 5 lbs of ballast in its payload bay. This prototype will allow for significant development and testing cost reductions and is actively being built by the MIT 16.82 students.

VIII. Aircraft Performance

This section details the endurance performance of the proposed long-endurance aircraft during off-design operations, predicted using the models created within the GPkit optimization framework. The off-design parameters considered are wind speed, payload weight, and payload power consumption.

A. Wind Speed vs. Endurance

We compare how different wind speeds during loiter affect the endurance of the aircraft. As shown in Figure 15, there are two flight patterns for the aircraft depending on the wind speed. Below a wind speed of 20 m/s, the aircraft will cruise at its maximum endurance speed of 20 m/s, and fly a standard racetrack holding pattern against the wind over the desired area. It means that the aircraft can loiter for up to 5.9 days in favorable (and nominal) wind conditions. Above 20 m/s, the aircraft will be flying directly into the wind and holding station in a hover, maintaining zero ground speed. The endurance of the aircraft drops below 5 days above 28 m/s winds.

B. Payload Weight vs. Endurance

Another performance study compares payload weight to endurance. The limiting factor on the payload weight of the aircraft is its longitudinal stability. The aircraft is designed to have a stability margin of 5% with a 10 lb payload, which presents a good compromise between static stability and low trim drag during loiter. The aircraft is able to accommodate higher payloads with the same static margin by allowing for the addition of lead ballast in the tail boom, which offsets the forward CG shift because of changes in payload mass. This allows the longitudinal control characteristics of the aircraft to stay similar regardless of the payload size.

Figure 16 shows the relationship between endurance and payload weight, assuming loiter at 25 m/s at 15,000 ft. The red line shows the ballast required at different payload weights, which increases linearly as would be expected. Because the structural margin of the aircraft decreases as the payload weight increases, it is recommended that the payload weight of the aircraft does not exceed 25 lbs. With a 25 lb payload, the aircraft has an endurance of 4.2 days.

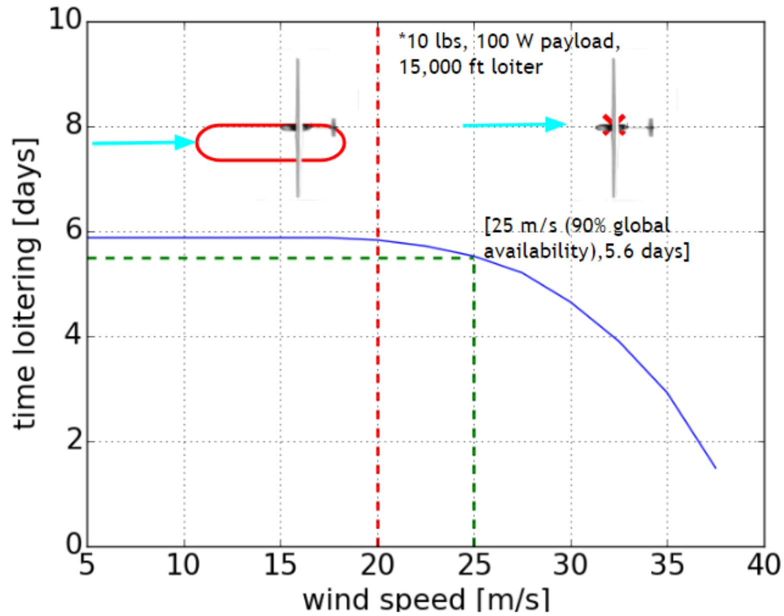

Figure 15: Performance curve of wind speed versus time on station. For wind speeds below 20 m/s (left of the red line) the plane will fly a holding pattern. For wind speeds greater than 20 m/s (right of the red line) the plane will fly directly into the wind, hovering over its station. The design point is shown in green.

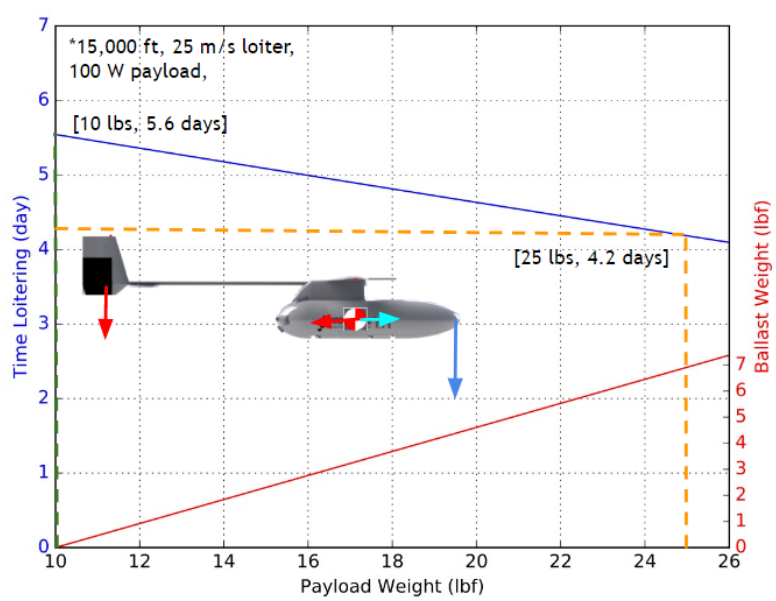

Figure 16: Performance curve of time on station versus payload weight. The aircraft is designed to fly with a 10 lb payload, but can accommodate up to 25 lbs. This assumes that the payload volume is constant at 1.43 ft^3 regardless of payload weight.

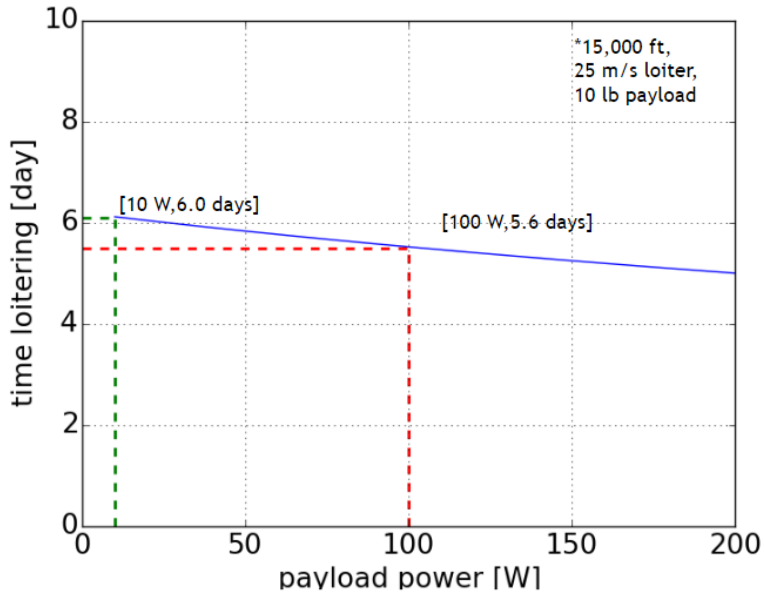

Figure 17: Performance curve of time on station versus payload power. The aircraft achieves 6.0 days of endurance with a 10W payload and 5.6 days with a 100W payload, assuming an 80% alternator efficiency.

C. Payload Power vs. Endurance

We examine the sensitivity of the aircraft endurance to the payload average power requirement, represented in Figure 17. As shown, the aircraft can achieve 6 days of endurance with a 10W payload. While the aircraft can fulfill higher power requirements, the increased power draw results in a decrease in endurance. With a 100W payload, the aircraft can station-keep for 5.6 days.

IX. Conclusion

This paper proposes a novel aircraft concept designed to keep small payloads (~10lbs) aloft for 5.6 days in a cost-effective and robust package. Although this aircraft exists in a niche currently unoccupied by existing aircraft, the technologies present in it are low-risk and largely proven. While this aircraft has persistent communication coverage as its primary mission, its modularity enables it to accommodate a variety of payloads of varying size, weight, and power. The construction of a prototype of the aircraft is underway at MIT, with a team of undergraduate and graduate students continuing work on the project as a part of the 16.82 Flight Systems Engineering Capstone subject. The project is being funded by MIT Lincoln Labs and the Air Force, with the goal of having a prototype by the end of May 2017.

X. Acknowledgements

The authors would like to thank their teammates in the 16.82 Flight Systems Engineering course at MIT who have worked, and are still striving to transform this aircraft from a concept into a working prototype. We would like to acknowledge the 16.82 course staff, teaching assistants, and Jennifer Craig for their assistance and guidance with this project, as well as Hanscom Air Force Base and MIT Lincoln Laboratory for their sponsorship and support.

XI. Appendix

A. Avionics

Some of the key technologies that enable this kind of long endurance MALE UAV come from avionics. The avionics for the aircraft is a lightweight and low power package that has sufficient robustness and redundancy to complete many 5.6 day missions. The system is capable of attitude determination and control, autonomous mission control, UHF and SATCOM communication, and airspace integration.

A fully functional avionics package that weighs 6.5 lbs and draws a mean power of 65 W has been designed. The avionics hardware can be separated into functional groups (see Figure 18) including sensors, control, central processing unit (CPU), communication, power management and extended items. These will be broken down below:

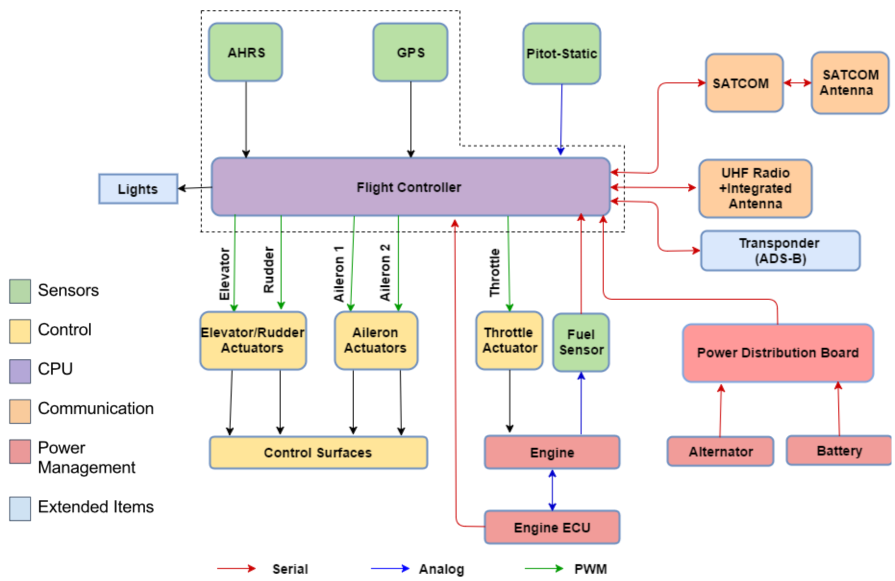

Figure 18: Avionics block diagram color-coded by functional area

- **Sensors:** The MicroPilot flight controller includes an on-board inertial navigation system. Other sensors include accelerometers, rate gyros, GPS, magnetometer, thermometer, and barometer. A pitot tube mounted on the wing provides the dynamic pressure, and two digital fuel sensors monitor fuel levels.
- **On-board computing:** The MicroPilot flight controller is the primary computer for autonomous control, mission decisions including switching flight phases, failsafe modes, LOS control through the UHF link and BLOS communication. It also provides pulse width modulation (PWM) outputs for the eight-servo aircraft control system.
- **Control:** Actuator sizing for a high endurance aircraft is a difficult task since servos tend to be the heaviest and most power hungry avionics components. The actuators specified for this aircraft were sized to have exceptional reliability, and also support control surface deflections at never-exceed speed at MSL.
- **Power distribution management:** The power distribution and management system is responsible for supplying all required onboard power needs. It consists of an alternator, battery, and Power Management Unit (PMU). For power generation, a Sullivan UAV S676-300F-01[9] alternator is specified.

At loiter conditions (4500 RPM), the alternator will be capable of delivering up to 214 W, satisfying all power requirements. An onboard 73 Wh lithium polymer battery provides fault-tolerance in the event of alternator or engine failure and ensures that high transient power loads do not cause momentary brown-outs. The battery's charge state is controlled by a battery management and power monitoring microcontroller, which submits diagnostic and monitoring information to the main flight computer.

- **Additional components** In order to comply with airspace integration requirements, the aircraft will include a Sagetech XPS-TR Mode S Transponder with Automatic Dependent Surveillance- Broadcast (ADS-B) Out. This transponder was chosen for its low size, weight, and power consumption as well as its capability of meeting the FAA's 2020 ADS-B requirements. Furthermore, there will be one light per wing (red on the port side and green on the starboard side) and a white strobe light on top.

- **Communication and ground station** The aircraft uses two modes of communication: a UHF two-way data radio for line-of-sight (LOS) and a satellite internet link (SATCOM) for beyond line-of-sight (BLOS). The ground station uses MicroPilot ground station control software, running on a laptop computer. Furthermore, for LOS control, a UHF radio controller is specified. Satellite communications capability is also required, and included in the ground station, to be able to contact Air Traffic Control in communications-denied areas.

The physical configuration of the avionics bay is shown in Figure 19.

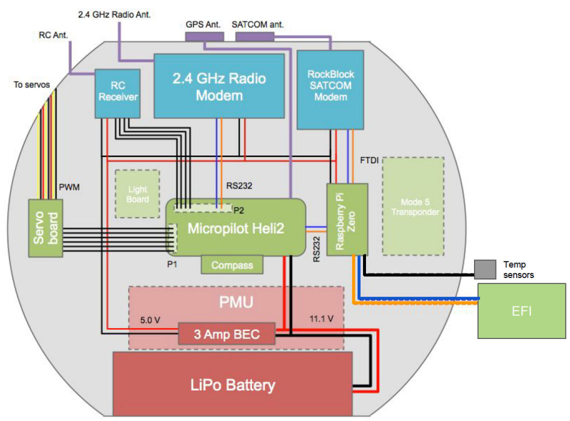

Figure 19: Physical layout of the avionics bay in front of the front bulkhead. Blue denotes communications, green control, red power system items.

B. Propulsion

There were two proposed engine options for the aircraft, which were the RCV Engines DF70, a two piston, four stroke engine, and the TorqPro TP70, a single piston, four stroke engine. Each of these engines meet both the propulsive and electric power requirements of the aircraft. The TP70 engine was chosen because of its significantly lower cost and shorter order lead time compared to its two-piston counterpart. The engine was ordered, and fitted with a COTS electronic fuel injection (EFI) system. Preliminary BSFC tests for the TP70 (shown in red in Figure 20) demonstrate similar performance characteristics for this engine compared to its counterpart (in blue; data obtained from manufacturer), validating the engine choice.

The engine runs on unleaded gasoline, with a 50:1 fuel/oil ratio. The fuel circuit is a conventional electronic fuel injection circuit, with a high pressure fuel pump drawing fuel from two main fuel tanks. A 22"x8" propeller was chosen by considering takeoff, top-of-climb and loiter thrust requirements. It was confirmed that the engine and propeller combination could meet the BSFC and thrust requirements at every phase of the mission.

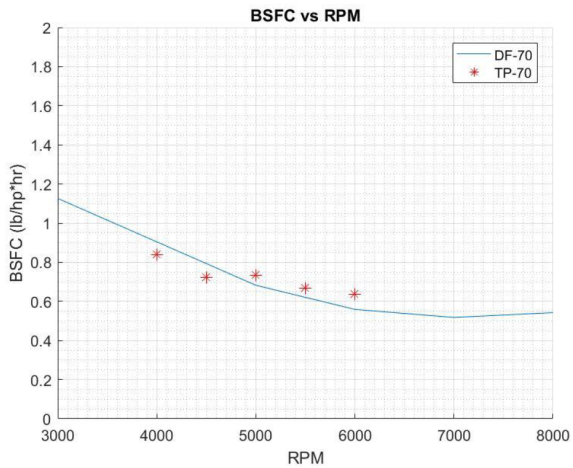

Figure 20: BSFC ground test data for the TP70, overlaid on the manufacturer-provided performance data for the DF70.

C. Modularity

With modularity in mind, the aircraft was designed to disassemble along breakpoints and fit within a 108"x24"x22" box for storage and transportation. This scheme is shown in Figure 21.

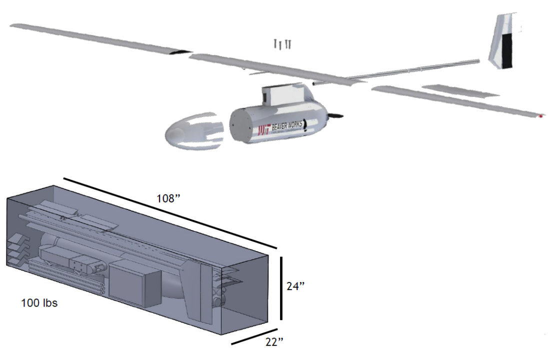

Figure 21: Aircraft breakpoints and packing configuration

References

[1]sUASNews Press, "Cost of flying Northrop's Global Hawk down over 50%," http://www.suasnews.com/2013/09/cost-of-flying-northrops-global-hawk-down-over-50-sources/, 09 2013.

[2]"Federation Aeronautique Internationale (FAI) Records," 2016.

[3]Wei, W. and Hansen, M., "Cost Economics of Aircraft Size," *Journal of Transport Economics and Policy*, Vol. 37, 2003, pp. 279–296.

[4]Hoburg, W. and Abbeel, P., "Geometric Programming for Aircraft Design Optimization," *AIAA*, 2014.

[5]Boyd, S., Kim, S.-J., Vanderberghe, L., and Hassibi, A., "A tutorial on geometric programming," 2007.

[6]Hoburg, W., Kirschen, P., and Abbeel., P., "Fitting geometric programming models to data," 2014.

[7]University of North Dakota, U. A. S. L., "Engine Reference," http://media.aero.und.edu/uasresearch.org/documents/195-197 Reference-Section Engines.pdf, feb 2016.

[8]Drela, M., "XFOIL Subsonic Airfoil Development System," http://web.mit.edu/drela/Public/web/xfoil/, 2013.

[9]Sullivan, "S676-300F-01 Alternator," .